

CHAPTER 6

THE EFFECT OF ANNEALING TREATMENT ON THE ELECTRICAL PROPERTIES AND PHASE TRANSITION OF B_2O_3 DOPED LEAD-FREE $Ba(Ti_{0.9}Sn_{0.1})O_3$ CERAMICS

In the present work, the posted sintered annealing method was applied for B_2O_3 doped $Ba(Ti_{0.9}Sn_{0.1})O_3$ ceramics. The ceramics were fabricated via a solid state reaction method: sintered at $1350^\circ C$ for 24h followed by annealing at $1100^\circ C$ for 4-32 h. Many electrical properties of the ceramics annealed at various annealing times were investigated with a variety of methods. Annealing for 4h produced a sharper phase transition with high dielectric constant. The high dielectric constant of 27,000 was recorded at ferroelectric to paraelectric phase transition temperature of $38^\circ C$. This sample also showed a high dielectric tunability of 70%. Ferroelectric performance of the sample was also improved. The improvements in electrical properties were related to the chemical homogeneity of the sample after annealing.

6.1 Introduction

Barium stannate titanate; $Ba(Ti_{1-x}Sn_x)O_3$ is one of an important ferroelectric materials [1]. The transition temperature from a ferroelectric (FE) to paraelectric (PE) phase of $Ba(Ti_{1-x}Sn_x)O_3$ can be varied by Sn concentration [2]. This material exhibits a high dielectric constant for $0.10 \leq x \leq 0.20$ compositions [3, 4]. For some compositions ($x > 0.2$), it shows a relaxor ferroelectric behavior [5]. A diffuse phase transition has been observed due to a partial isovalent substitution of Ti^{4+} by Sn^{4+} [6].

Recently, the dielectric constant of $\text{Ba}(\text{Ti}_{0.9}\text{Sn}_{0.1})\text{O}_3$ system can be enhanced by adding B_2O_3 in some concentration. Increasing B_2O_3 concentration has a strong effect on the dielectric phase transformation [7].

However, it is believed that chemical heterogeneity in ceramic can occur after processing, which may reduce the optimal properties. To reduce this effect, thermal annealing is an effective method for decreasing chemical heterogeneity and in further optimizing the electrical properties. Many authors have studied the effect of annealing temperature and time on dielectric and ferroelectric properties in various perovskite type ceramics such as; PZT-PZN [8] and PZN-PT-BT [9].

In this work, we applied this method to B_2O_3 -doped $\text{Ba}(\text{Ti}_{0.9}\text{Sn}_{0.1})\text{O}_3$ ceramics system. It is expected that the annealing treatment should produced an improvement in densification and the electrical properties of this ceramics.

6.2 Experimental

$\text{Ba}(\text{Ti}_{1-x}\text{Sn}_x)\text{O}_3$ powders with a stoichiometric composition of $\text{Ba}(\text{Ti}_{0.9}\text{Sn}_{0.1})\text{O}_3$ were prepared using the conventional solid-state method with reagent grade BaCO_3 , SnO_2 and TiO_2 . The starting powders were mixed and milled in isopropanol for 24h using a zirconia grinding media. The mixture was dried at 120°C and calcined at 1300°C for 2h. B_2O_3 powder, equivalent to 1.0 wt%, was then blended to calcined powder. An organic binder of polyvinyl alcohol was also added into the mixed powders and then ball-milled in isopropanol for 24 h. This slurry was dried at 120°C and sieved to form a homogeneous powder which was pressed at 100 MPa into 15

mm diameter pellets. The obtained pellets were sintered at 1350°C for 4 h. After sintering, the ceramics were annealed at 1100°C for 4-32 h.

X-ray diffraction technique was used to observe the phase formation before and after annealing. The density of the sintered ceramics was measured using the Archimedes' method. For the electrical characterization, fired-on silver electrodes were applied to the pellets which had been ground to a thickness of 1.0 mm. Dielectric measurements were carried out using an impedance analyzer over the range of 1 kHz to 1 MHz and temperatures from -20 to 100°C.

6.3 Results and discussion

The XRD patterns for the ceramics annealed at various times are shown in Figure 6.1. The XRD results revealed that all samples exhibited a solid solution with a perovskite phase. There was small amount of impurity product in the XRD patterns for the annealed samples.

Figure 6.2 shows the variations of the dielectric constant as a function of temperature in the frequency range of 1 kHz to 1MHz for the present ceramics. The dielectric data revealed that the annealing has a significant effect on the dielectric constant.

The values of the dielectric constant at the dielectric peak ($\epsilon_{r,\max}$) as a function of annealing time are shown in Figure 6.3. An improvement of dielectric constant was observed. The value of $\epsilon_{r,\max}$ (at 1kHz) increased from 13,800 for the as-sintered sample to 28,100 for the 4h sample and then decreased with further annealing times.

Loss tangent as a function of temperature and frequency plots are also illustrated in Figure 6.2. The loss tangent behavior did not change significantly with changing annealing time. The loss tangent decreased with increasing frequency. However, the values of loss tangent were lower than 0.10 for all sample between -20°C to 100°C.

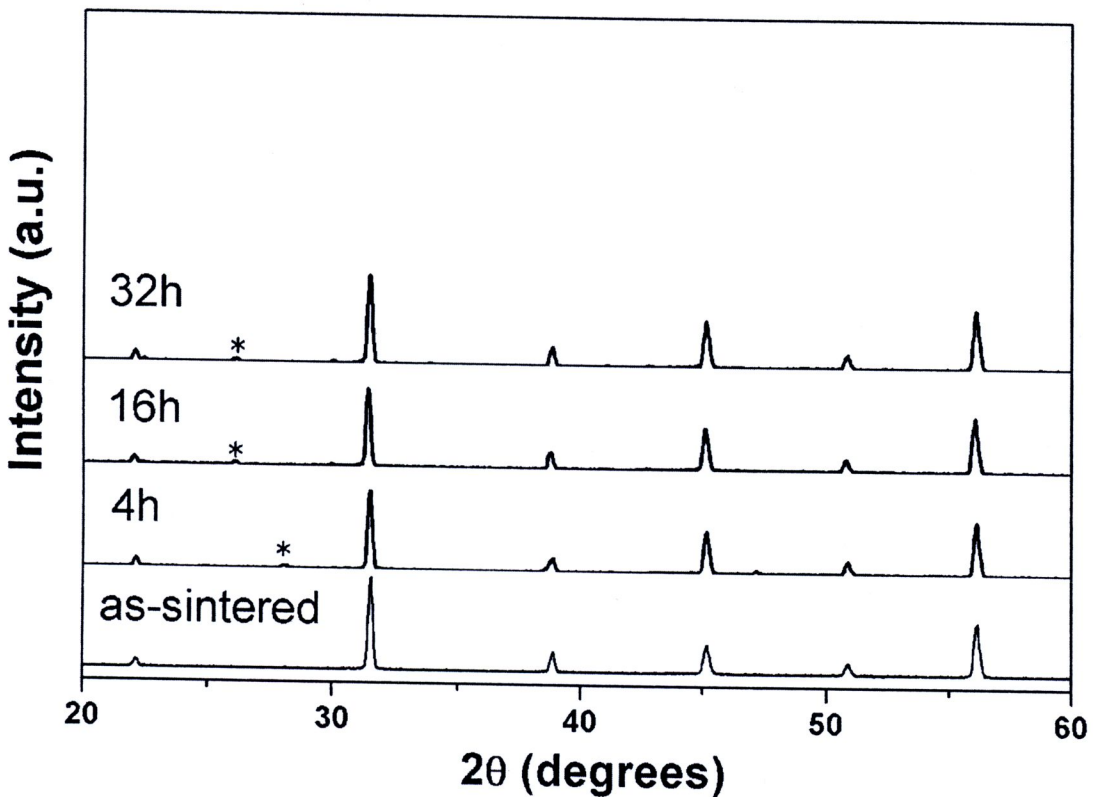


Figure 6. 1 X-ray powder diffraction patterns of BTS10 - 1 wt.% B₂O₃ at room temperature as a function of annealing time. Impurity phases are indicated by (*).

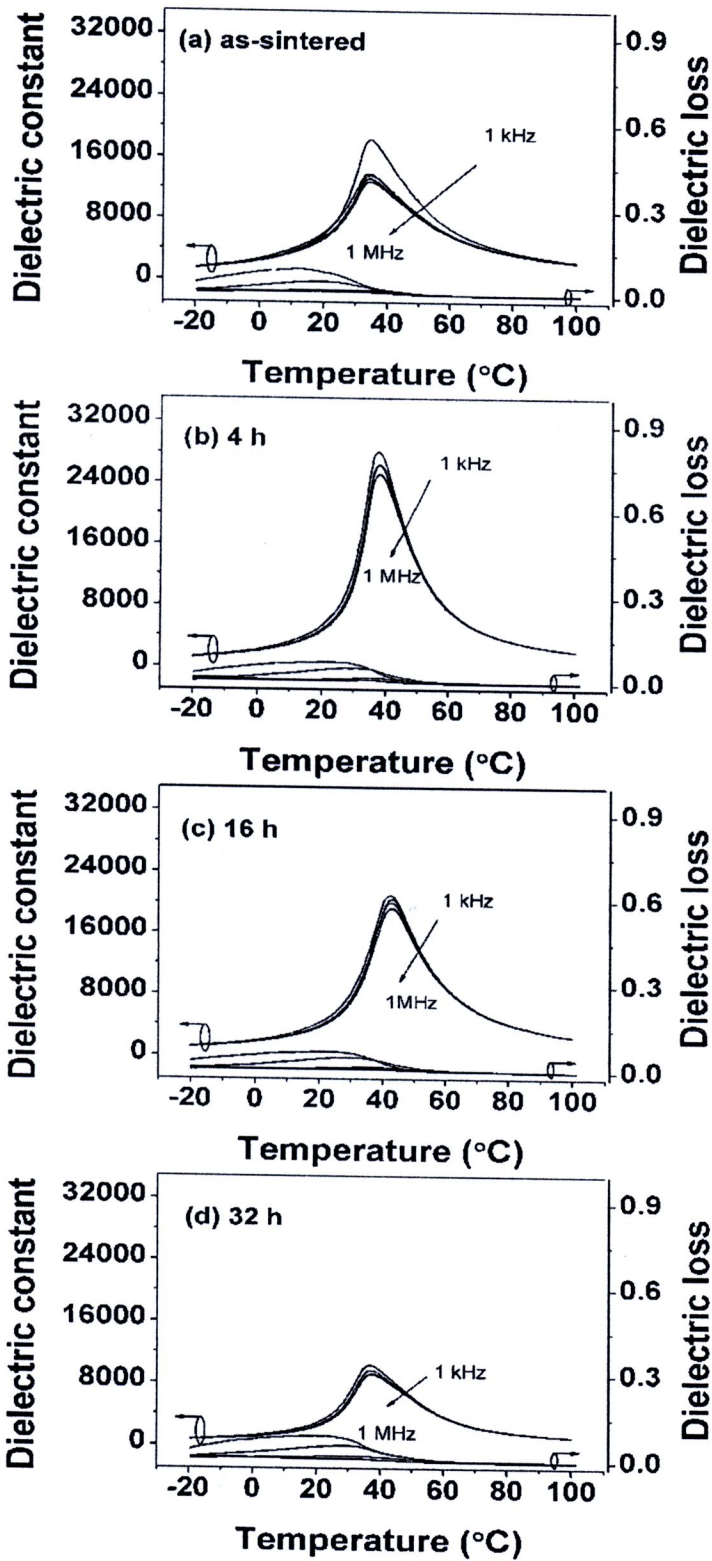


Figure 6. 2 (a)-(d) Variation of the dielectric constant and loss with temperature and frequency for the ceramics annealing at various times.

A plot of transition temperature (T_m) versus annealing time is shown in Figure 6.3. The T_m at the dielectric peak increased from 35°C for the as-sintered sample to 42°C for the 16h annealed sample and then decreased to 37°C for the 32h annealed sample. Further, the as-sintered sample showed a diffuse phase transition. After annealing, however, a sharp phase transition was observed especially for the 4h annealed sample.

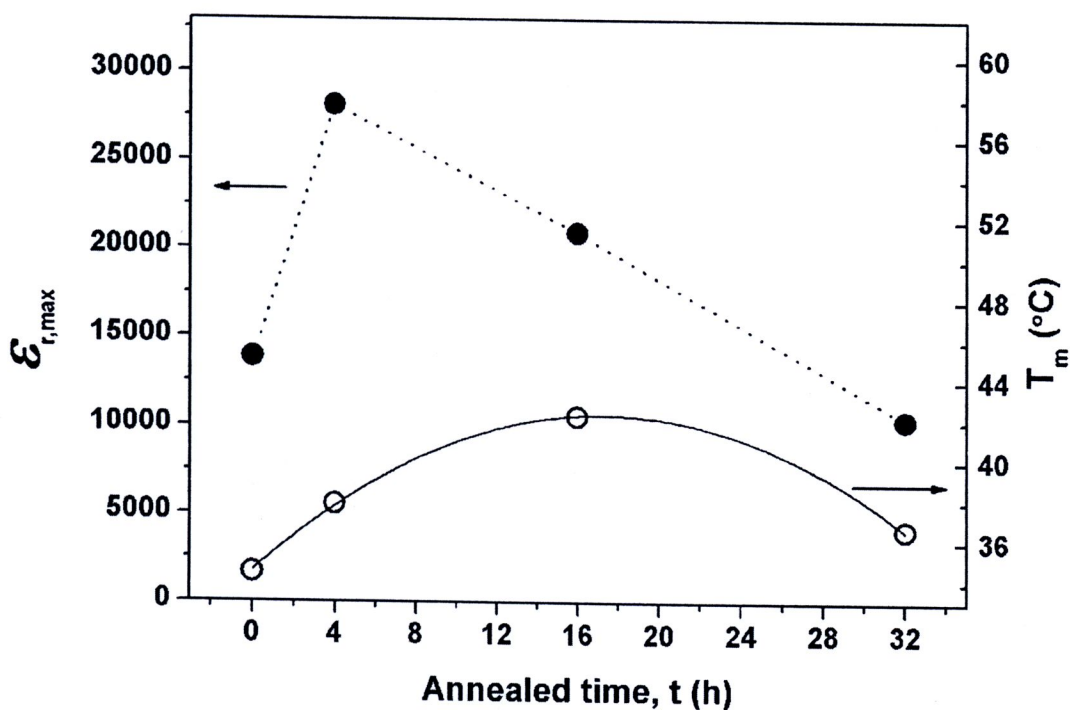


Figure 6. 3 The maximum dielectric constant and transition temperature of BTS10-1wt% B_2O_3 as a function of annealing time.

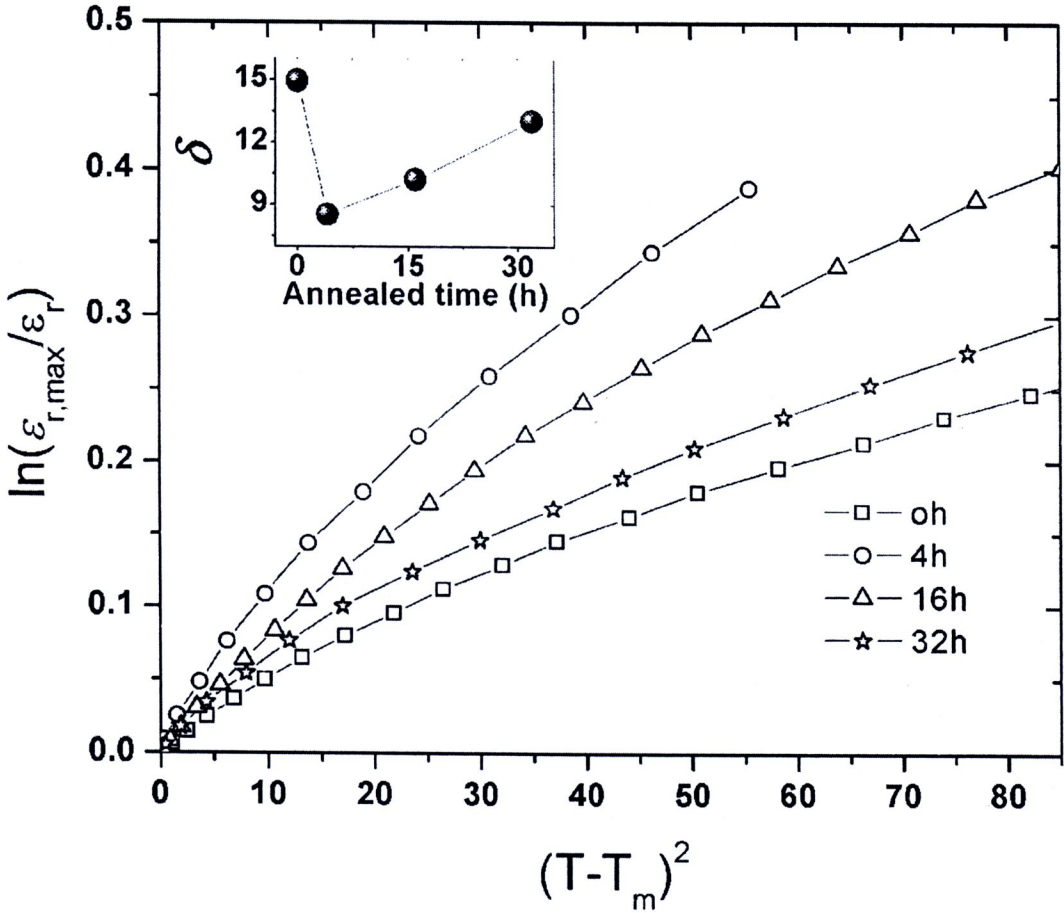


Figure 6. 4 Quadratic dependence of temperature on logarithmic dielectric of the samples at 1 kHz as a function of annealing time.

In order to measure the degree of the diffuse phase transition (in contrast to sharp phase transition), diffuseness parameter (δ_γ) was determined using the following expression [10]:

$$\frac{\epsilon_{r,max}}{\epsilon_r} = \exp\left[\frac{(T - T_m)^2}{2\delta_\gamma^2}\right] \quad (6.1)$$

where $\epsilon_{r,max}$ is maximum value of the dielectric constant at T_m and δ_γ is the dielectric constant of sample. The value of δ_γ can be obtained from the $\ln(\epsilon_{r,max}/\epsilon_r)$ versus the $(T$

$-T_m)^2$ curve [11], as seen in Figure 6.4. This value is valid for the range of $(\epsilon_{r,max}/\epsilon_r) < 1.5$, as shown by Pilgrim et al. [10].

The values of parameter δ_γ at various annealing time are displayed in the inset of Figure 6.4. The δ_γ was laid between 8 and 15°C and the lowest value of δ_γ was observed for the 4h annealed sample, indicating that annealing for 4h promoted a sharper phase transition in the ceramics.

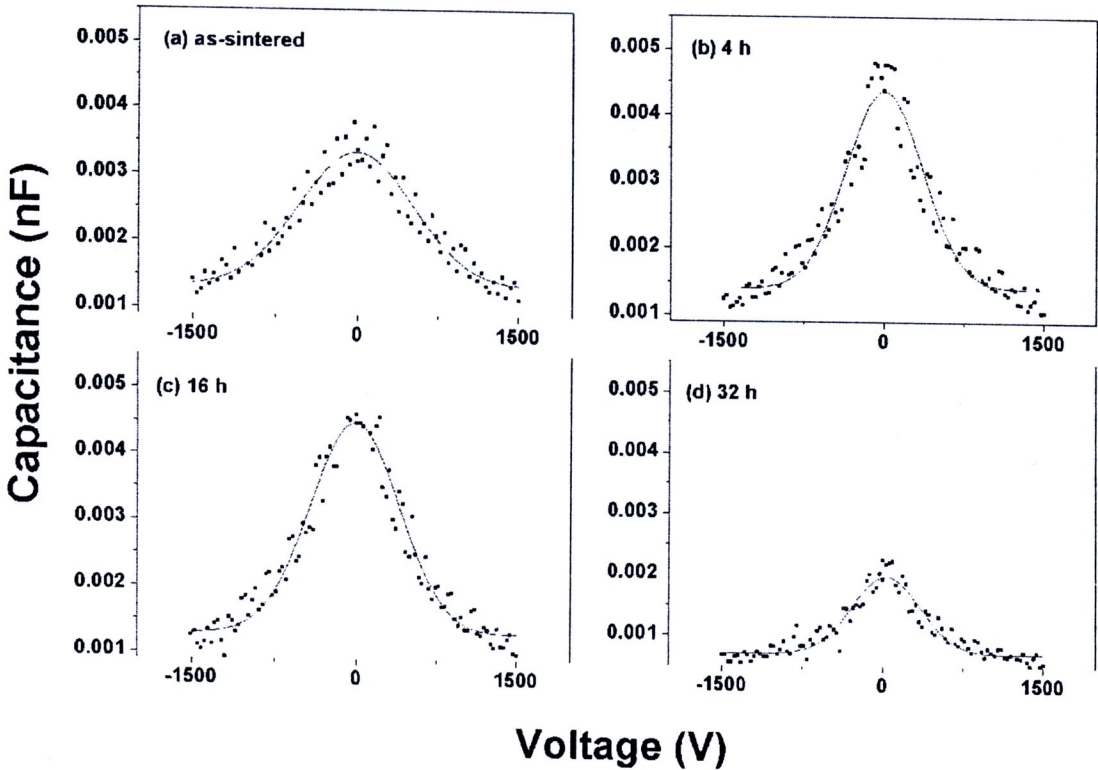


Figure 6. 5 Capacitance-applied voltage characteristics of the ceramics annealed at various times.

The Capacitance (C) versus applied electric field (E) plots for the ceramics annealed at various temperatures are shown in Figure 6.5. High tunability was

observed for the present ceramics. Generally, the relative tunability (n_r) can be defined as [12]:

$$n_r(\%) = \left(\frac{\epsilon_r(0) - \epsilon_r(E)}{\epsilon_r(0)} \right) \times 100 \quad (6.2)$$

where $\epsilon_r(0)$ and $\epsilon_r(E)$ are the dielectric constant at zero and applied electric field E .

Plot of n_r versus annealing time is shown in Figure 6.6. The values of n_r were in a range of 60-76%, and the 4h annealed sample showed the highest relative tunability ($\sim 76\%$).

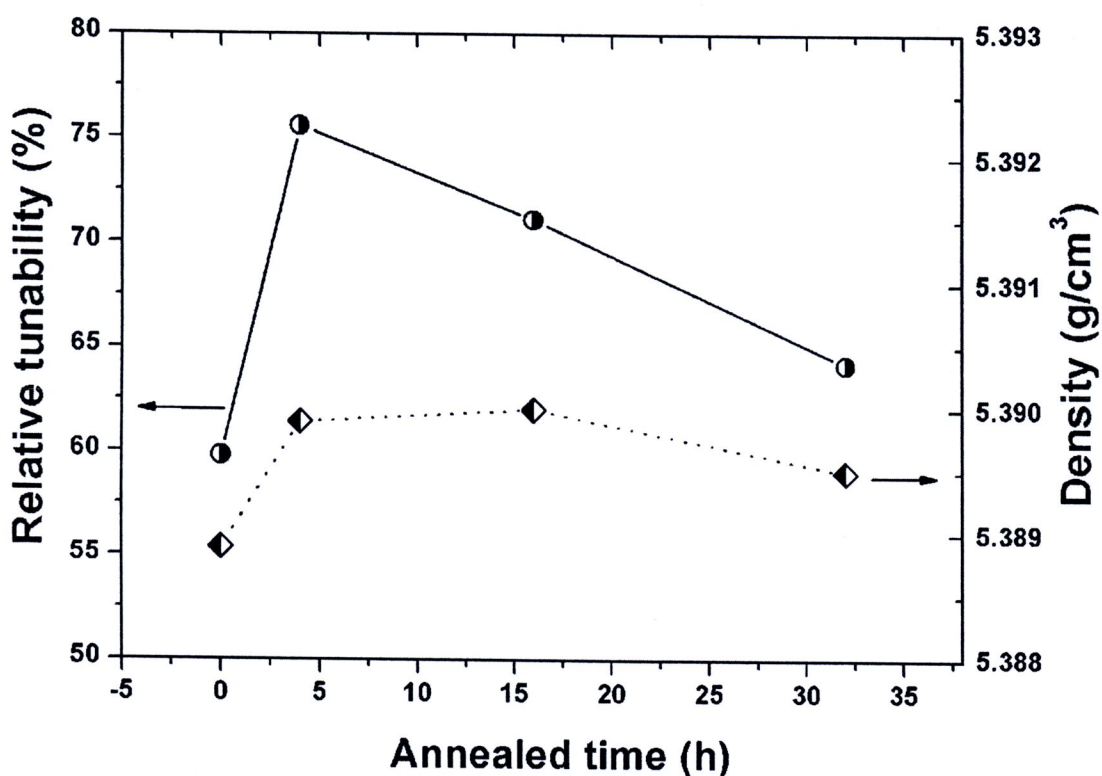


Figure 6. 6 Relative tunability and density as a function of annealing time of the samples.

Polarization hysteresis (P - E loop) measured at room temperature were performed using a Sawyer–Tower circuit. The ferroelectric hysteresis loops for as-sintered and annealed samples are shown in Figure 6.7. The result revealed that all samples exhibited a ferroelectric behavior.

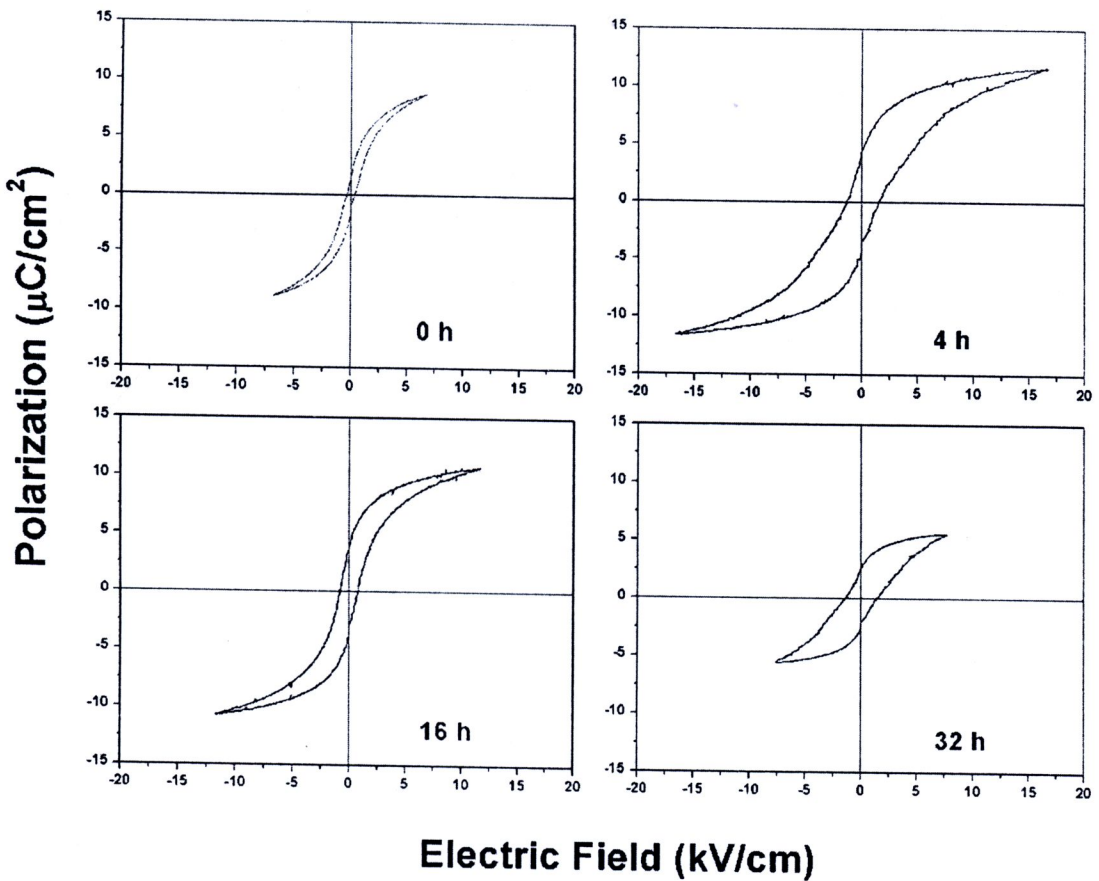


Figure 6. 7 Dependence of the polarization versus electric field (P - E) loop of the samples.

The value of remnant polarization (P_r) increases from $1.6 \text{ } \mu\text{C}/\text{cm}^2$ for the as-sintered sample to $4.3 \text{ } \mu\text{C}/\text{cm}^2$ for the 4h sample and then slightly decreases for the increased annealing time of 32h. There was systematic dependence of the coercive

field (E_c) on the annealing time. And, the values of E_c were in the range of 0.3-1.4 kV/cm. Values of P_r and the E_c as a function of annealing time are displayed in Figure 6.8.

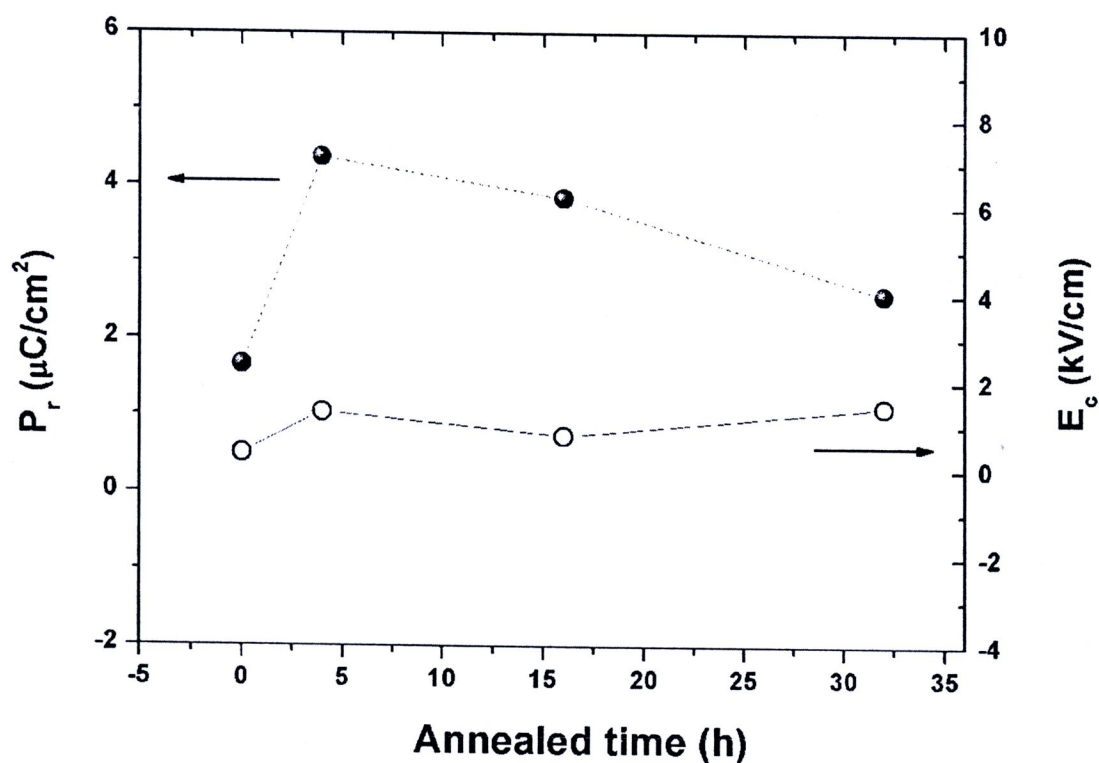


Figure 6. 8 Variation of remanent polarization, P_r and coercive field, E_c of ceramics annealed at various times.

In the present work, the density of the samples was also determined. The result is shown in Figure 6.6. The density increased from $5.3889 \text{ g}/\text{cm}^3$ for the as-sintered sample to $5.3900 \text{ g}/\text{cm}^3$ for the 16h annealed sample then slightly decreased to $5.3895 \text{ g}/\text{cm}^3$ for the 32h annealed samples. It should be noted that the density for the 4h annealed sample was $5.3899 \text{ g}/\text{cm}^3$ which is comparable to the value of the 16h

annealed sample. Hence, the improvement in densification is not an important reason for the improvements of the electrical properties.

It was reported that adding of B_2O_3 in $Ba(Ti_{0.9}Sn_{0.1})O_3$ resulted in the improvement in dielectric constant [13]. However, the addition may cause a chemical heterogeneity in the samples since BTS10 has a complex structure, comparing to $BaTiO_3$ (a prototypic ferroelectric material). Therefore, it is believed that the decreasing of chemical heterogeneity in the samples after annealing may be a main reason for the improvements in many electrical properties for the present work.

6.4 Conclusions

The ceramics of BTS10 doped with 1 wt.% of B_2O_3 were fabricated by a solid-state method. The ceramics were annealed for various times. The improvements of many electrical properties such as dielectric constant, tunability, and ferroelectric were observed. It is proposed that the improvements can be related to the decrease of chemical heterogeneity in the samples after annealing. This method may be an effective method for improving the electrical properties of other lead free ceramics.

6.5 References

- [1] A.J. Moulson, J.M. Herbert, Wiley InterScience (Online service), *Electroceramics : materials, properties, applications*, in, J. Wiley,, New York, 2003, pp. 557 p. ill.

- [2] J.N. Lin, T.B. Wu, Effects of isovalent substitutions on lattice softening and transition character of BaTiO₃ solid solutions, *Journal of Applied Physics*, 68 (1990) 985-993.
- [3] S. Markovic, M. Mitric, N. Cvjeticanin, D. Uskokovic, Preparation and properties of BaTi_{1-x}Sn_xO₃ multilayered ceramics, *Journal of the European Ceramic Society*, 27 (2007) 505-509.
- [4] X. Wei, X. Yao, Preparation, structure and dielectric property of barium stannate titanate ceramics, *Materials Science and Engineering: B*, 137 (2007) 184-188.
- [5] V.V. Shvartsman, J. Dec, Z.K. Xu, J. Banys, P. Keburis, W. Kleemann, Crossover from ferroelectric to relaxor behavior in BaTi_{1-x}Sn_xO₃ solid solutions, *Phase Transitions*, 81 (2008) 1013-1021.
- [6] W. Xiaoyong, F. Yujun, Y. Xi, Dielectric relaxation behavior in barium stannate titanate ferroelectric ceramics with diffused phase transition, *Applied Physics Letters*, 83 (2003) 2031-2033.
- [7] C.R.K. Mohan, P.K. Bajpai, Effect of sintering optimization on the electrical properties of bulk Ba_xSr_{1-x}TiO₃ ceramics, *Physica B: Condensed Matter*, 403 (2008) 2173-2188.
- [8] N. Vittayakorn, G. Rujijanagul, D.P. Cann, The improvement in dielectric and ferroelectric performance of PZT-PZN ceramics by thermal treatment, *Current Applied Physics*, 7 (2007) 582-585.
- [9] A. Halliyal, U. Kumar, R.E. Newnham, L.E. Cross, Dielectric and ferroelectric properties of ceramics in the Pb(Zn_{1/3}Nb_{2/3})O₃-BaTiO₃-PbTiO₃ System, *Journal of the American Ceramic Society*, 70 (1987) 119-124.

- [10] S.M. Pilgrim, A.E. Sutherland, S.R. Winzer, Diffuseness as a useful parameter for relaxor ceramics, *Journal of the American Ceramic Society*, 73 (1990) 3122-3125.
- [11] G. Rujijanagul, N. Vittayakorn, Influence of fabrication processing on phase transition and electrical properties of $0.8\text{Pb}(\text{Zr}_{1/2}\text{Ti}_{1/2})\text{O}_3$ - $0.2\text{Pb}(\text{Ni}_{1/3}\text{Nb}_{2/3})\text{O}_3$ ceramics, *Current Applied Physics*, 8 (2008) 88-92.
- [12] J. Venkatesh, V. Sherman, N. Setter, Synthesis and dielectric characterization of potassium niobate tantalate ceramics, *Journal of the American Ceramic Society*, 88 (2005) 3397-3404.
- [13] N. Tawichai, U. Intatha, S. Eitssayeam, K. Pengpat, G. Rujijanagul, T. Tunkasiri, Influence of B_2O_3 on electrical properties and phase transition of lead-free $\text{Ba}(\text{Ti}_{0.9}\text{Sn}_{0.1})\text{O}_3$ ceramics, *Phase Transitions*, 83 (2010) 55-63.